

Locating damaged storeys in a shear building based on its sub-structural natural frequencies

W.C. Su^a, C.S. Huang^{b,*}, S.L. Hung^b, L.J. Chen^b, W.J. Lin^b

^a National Center for High Performance Computing, Hsinchu 30050, Taiwan

^b National Chiao Tung University, Hsinchu 30050, Taiwan

ARTICLE INFO

Article history:

Received 3 August 2011

Revised 1 February 2012

Accepted 2 February 2012

Available online 22 March 2012

Keywords:

Damage diagnosis

Wavelet transform

Sub-structural frequencies

Shear building

ABSTRACT

Vibration-based damage detection methods are simple and conventionally adopted to monitor the structural health of buildings. This work proposes a simple and efficient approach to locating the storeys whose properties (stiffness and mass) change in the life cycle of a shear building. The storeys that may be damaged are determined by comparing the natural frequencies of sub-structures in different stages in the life cycle of a building. An appropriate ARX (autoregressive with exogenous input) model of a sub-structure of a shear building is established from the sub-structural dynamic responses in terms of acceleration or velocity. The parameters in an ARX model of a sub-structure are identified through the continuous wavelet transform, and the natural frequency and damping ratio of the sub-structure are estimated directly through these identified parameters. The effectiveness of the proposed procedure is verified using the numerically simulated earthquake acceleration responses and ambient vibration responses of a six-storey shear building that is damaged at one or two storeys with different damage levels. The effect of noise on the accuracy of the proposed approach is also examined. The proposed scheme is demonstrated to be superior to COMAC (Coordinate Modal Assurance Criterion) and the frequency response function curvature method in identifying damaged storeys. The proposed method is also applied to process the dynamic responses of three five-storey steel frames, which are not shear buildings, in shaking table tests. The differences in the floor mass or storey stiffness among these frames are accurately reflected in the sub-structural natural frequencies that are obtained by the proposed approach.

© 2012 Elsevier Ltd. All rights reserved.

1. Introduction

A structure may sustain damage either when subjected to severe loading, such as a strong earthquake, or when its material is degraded. The serviceability and safety of structures depend on the detection and location of structural damage. Early detection of structural degradation can prevent catastrophic failure. Research on structural health monitoring has been expanding rapidly over the last two decades.

Reviews of the literature [1–8] agree that vibration-based damage detection methods are simple and widely adopted. Vibration-based damage detection methods utilize the dynamic characteristics (modal frequencies, damping ratios, and modal shapes) of a whole structure. These dynamic characteristics of a structure are known to be functions of its stiffness or mass distribution, and are identified from its dynamic responses. Theoretically, changes in stiffness and mass of a structure should lead to changes

in its dynamic characteristics. Cawley and Adams [9], Hearn and Tesla [10], Friswell et al. [11], Messina et al. [12], and Zapico and González [13] presented various methods that exploit the modal frequencies of full structures to detect damage. These methods are not very effective because modal frequencies mainly depend on the global behaviors of the structure, whereas damage is a rather local phenomenon. Some indexes that are based on modal shapes have been proposed. They include such as MAC (Modal Assurance Criterion) [14,15], COMAC (Coordinate Modal Assurance Criterion) [15–17], MSE (Modal Strain Energy) [18–21], EEQ (Elemental Energy Quotient) [22], and EMSEC (Elemental Modal Strain Energy Change) [23,24]. Although MAC and COMAC are easy to apply, they are not very sensitive to the existence of damage. To estimate the MSE, EEQ and EMSEC for a damaged structure, the stiffness matrix of the structure in undamaged state, which is difficult to accurately determine, is needed. Pandey et al. [25] employed curvature mode shapes to locate damage in a beam, and Sampaio et al. [26] further proposed FRFCM (frequency response function curvature method) and evaluated the efficiency of this method using numerically simulated data and experimental data for a real bridge. Using modal frequencies and modal shapes, Lin [27] and Pandey and Biswas [28] established flexibility matrices of a structure in undamaged

* Corresponding author. Tel.: +886 3 5712121x54962; fax: +886 3 5716257.

E-mail addresses: wichcv86@gmail.com (W.C. Su), cshuang@mail.nctu.edu.tw (C.S. Huang), slhung@mail.nctu.edu.tw (S.L. Hung), Linkchen59@yahoo.com (L.J. Chen), Yolanda.cv97g@nctu.edu.tw (W.J. Lin).

and damaged states, and located damage by considering changes in the components of the flexibility matrices. Patjawit and Kanok-Nukulchai [29] further developed a global flexibility index to infer the degradation of highway bridges.

As complex systems, civil structures normally have substantial redundancy, and are modeled with a large number of degrees of freedom (DOFs). Practical limitations allow only a limited number of sensors to be installed in a structural health monitoring system, and the measured responses do not yield information about all of the degrees of freedom of the structures. Using these incomplete measurements to determine important parameters of a full structure may not provide a unique solution. To solve these problems, sub-structural identification techniques have been proposed. Koh et al. [30] adapted the extended Kalman filter by adding a weighted global iteration algorithm to determine the stiffness matrix and the damping matrix of a sub-structure through solving the state and observation equations of the sub-structure. This approach needs acceleration, velocity and displacement responses of the sub-structures under consideration. There is not an efficient way to accurately measure displacement responses of a structure under earthquake. The displacement responses required in an identification method are typically obtained from integrating measured acceleration or velocity responses, and an appropriate integration scheme must be carefully used. This approach was further modified to use acceleration responses only in [31], where a non-classical approach of genetic algorithms was applied. Zhao et al. [32] estimated the stiffness matrix and the damping matrix of a sub-structure in the frequency domain using an iteration algorithm. Yun and Bahng [33] evaluated sub-structural parameters using a back-propagation neural network, with modal data as inputs and sub-matrix scaling factors as outputs. This approach assumes the availability of the mass matrix. Yun et al. [34] extended their approach [33] to estimate the joint damages of a steel structure. Huang and Yang [35] developed an adaptive damage tracking technique for sub-structures, known as sequential nonlinear least-square estimation with unknown inputs and unknown outputs. It is a recursive approach, whose accuracy is sensitive to noise in the measured data. They considered only 2% noise, which is usually too low in a real application.

The dynamic behaviors of a building differ markedly from those of other structures. The assumption of rigid floors is valid for most buildings and three DOFs (two horizontal displacement components and one torsion angle) are needed to describe the horizontal motions of each floor in an earthquake. When a building is symmetrical, the horizontal displacement components and torsion angle of each floor are uncoupled. Moreover, if the bending of beam and the effect of axial force on column stiffness are neglected, the behaviors of a symmetrical building are close to those of a shear building model considered here. Accordingly, the building can be divided into numerous sub-structures, including only two or three floors, and the availability of measurements on the sub-structures of interest can be reasonably assumed.

This work presents a simple and efficient approach for determining the storeys of a shear building whose properties change. This work establishes sub-structural ARX (autoregressive with exogenous input) models from the dynamic responses of various sub-structures of a shear building to estimate their natural frequencies. The measured responses are in terms of acceleration or velocity. The acceleration responses are used herein. Then, the sub-structural natural frequencies in the reference stage (without damage) are compared with those in the current stage (possibly damaged), to locate easily any damaged storeys. The sub-structural ARX models are developed via the continuous wavelet transform. Although the natural frequencies of an entire building represent global behaviors, those of its sub-structures reflect local behaviors.

The proposed procedure is validated using the numerically simulated earthquake acceleration responses and ambient vibration velocity responses of a six-storey shear building. A series of cases, involving various degrees of single-site and dual-site damage, is examined. The effect of noise on diagnosis of the damage of the building is also investigated. Then, the proposed approach is further applied to the dynamic responses of three five-storey steel frames in shaking table tests. These frames are not shear buildings. Their fourth storeys may have a different mass or stiffness from the other storeys. One of the frames was shaken under a small and a large earthquake inputs, such that it responded linearly in the small earthquake, and its columns in the first storey yielded in the large earthquake. The differences between the frames are captured by the sub-structural natural frequencies that are evaluated by the proposed approach. For comparison, MAC is also adopted for damage detection, and COMAC and a frequency response function curvature method-based index [26] are also employed to locate the damaged storeys.

2. Evaluation of modal parameters by wavelet transform

The equations of motion of a linear structure are,

$$\mathbf{M}\ddot{\mathbf{x}} + \mathbf{C}\dot{\mathbf{x}} + \mathbf{K}\mathbf{x} = \mathbf{f}, \quad (1)$$

where \mathbf{M} , \mathbf{C} and \mathbf{K} are mass, damping, and stiffness matrices, respectively; $\ddot{\mathbf{x}}$, $\dot{\mathbf{x}}$ and \mathbf{x} are the acceleration, velocity and displacement response vectors of the system; and \mathbf{f} is the input force vector. Eq. (1) can be discretized as [36]

$$\mathbf{y}(t) = \sum_{i=1}^I \Phi_i \mathbf{y}(t-i) + \sum_{j=0}^J \Theta_j \mathbf{f}(t-j), \quad (2)$$

where $\mathbf{y}(t-i)$ and $\mathbf{f}(t-i)$ are the measured responses, in terms of acceleration, velocity or displacement, and the forces at time $t-i\Delta t$, respectively; I and J denote the lags of output and input, respectively, Φ_i and Θ_j are coefficient matrices. Notably, Eq. (2) is the time series model ARX with multiple variables without noise terms, and shows the relations between output vector \mathbf{y} and input vector \mathbf{f} . Huang [36] demonstrated that I and J theoretically equal two when the acceleration responses without noise for all degrees of freedom are used to establish Eq. (2). When incomplete measurements with noise are utilized to develop Eq. (2), I and J of larger than two should be used.

Treating $\mathbf{y}(t-i)$ and $\mathbf{f}(t-i)$ as vector functions, and applying the continuous wavelet transform to Eq. (2) yields

$$W_\psi \mathbf{y}(a, \bar{b}) = \sum_{i=1}^I \Phi_i W_\psi \mathbf{y}(a, \bar{b}-i) + \sum_{j=0}^J \Theta_j W_\psi \mathbf{f}(a, \bar{b}-j), \quad (3)$$

where the continuous wavelet transform of a function $f(t)$ is defined as

$$W_\psi f(a, b) = \frac{1}{\sqrt{a}} \int_{-\infty}^{\infty} f(t) \psi^* \left(\frac{t-b}{a} \right) dt, \quad (4)$$

the superscript $*$ denotes the complex conjugate; a is a dilation or scale parameter; b is a translation parameter, and $\psi(t)$ is a mother wavelet function. The translation parameter b is set to $\bar{b}\Delta t$, and \bar{b} is an integer because b must be a discrete number when the transformation is applied to discrete responses.

One can obtain the following equations in matrix form from Eq. (3) with various \bar{b} ,

$$[\mathbf{Y}^{(0)}] = [\hat{\mathbf{C}}] \begin{bmatrix} \mathbf{Y} \\ \mathbf{F} \end{bmatrix}, \quad (5)$$

where

Table 1

Descriptions of simulated damage cases.

No. of damage case	Description of damage case
1	Reduce 10% of k_1 at first storey
2	Reduce 20% of k_1 at first storey
3	Reduce 10% of k_5 at fifth storey
4	Reduce 20% of k_5 at fifth storey
5	Reduce 10% of k_1 & 10% of k_4
6	Reduce 10% of k_1 & 20% of k_4
7	Reduce 10% of k_4 & 10% of k_5
8	Reduce 20% of k_4 & 10% of k_5

$$m_1\ddot{x}_1 + c_{11}\dot{x}_1 + k_1x_1 = f_1 - c_{21}\dot{x}_2^r + k_2x_2^r \quad \text{for } j = 1 \quad (12c)$$

where $x_j^r = x_j - x_{j-1}$. If an MISO ARX model with \ddot{x}_j^r as output and f_j , \ddot{x}_{j-1} and \ddot{x}_{j+1}^r as inputs is constructed for each $j = 2$ to $(n - 1)$, then the natural frequency of the j th sub-structure, which is theoretically $\sqrt{k_j/m_j}$ (Hz), should be determinable. Consequently, establishing an ARX model equivalent to Eq. (12b) is better than finding an equivalent ARX model equivalent to Eq. (11) in locating the damaged storeys because a change in k_j alters the natural frequency given by Eq. (12b) more than that given by Eq. (11).

A significant problem arises in establishing an MISO ARX model that is equivalent to Eq. (12b) with $j = n - 1$ from the earthquake responses or free vibration responses. For a building in an earthquake, $f_n = -m_n a_g$ and $f_{n-1} = -m_{n-1} a_g$ where a_g is the base excitation

acceleration. An ARX model with \ddot{x}_{n-1}^r as an output and a_g , \ddot{x}_{n-2} and \ddot{x}_n^r as inputs is not uniquely related to Eq. (12b). From Eqs. (12a) and (12b) with $j = n - 1$ one can obtain

$$\begin{aligned} (m_{n-1} + m_n)\ddot{x}_{n-1}^r + (c_{(n-1)(n-1)} + c_{nn} + 2c_{n(n-1)})\dot{x}_{n-1}^r + k_{n-1}x_{n-1}^r \\ = -(m_n + m_{n-1})\ddot{x}_g - (m_{n-1} + m_n)\ddot{x}_{n-2} - (c_{nn} + 2c_{n(n-1)} \\ + c_{(n-1)(n-1)} + c_{(n-1)(n-2)})\dot{x}_{n-2} - m_n\ddot{x}_n^r + (c_{n(n-1)} - c_{nn})\dot{x}_n^r \end{aligned} \quad (13)$$

Twice differentiating Eq. (12b) with $j = n - 1$ and Eq. (13) with respect to t and discretizing the resulting equations by a typical central difference technique yield, respectively,

$$\ddot{x}_{n-1}^r(t) = \sum_{i=1}^2 \tilde{\phi}_i \ddot{x}_{n-1}^r(t-i) + \sum_{j=0}^2 \tilde{\theta}_j \ddot{y}(t-j) \quad (14)$$

$$\ddot{x}_{n-1}^r(t) = \sum_{i=1}^2 \tilde{\phi}_i \ddot{x}_{n-1}^r(t-i) + \sum_{j=0}^2 \tilde{\theta}_j \ddot{y}(t-j) \quad (15)$$

$$\text{where } \tilde{\phi}_1 = \frac{1}{\tilde{\alpha}} \left(\frac{2m_{n-1}}{\Delta t^2} - k_{n-1} \right),$$

$$\tilde{\phi}_2 = -\frac{1}{\tilde{\alpha}} \left(\frac{m_{n-1}}{\Delta t^2} - \frac{c_{(n-1)(n-1)} + c_{n(n-1)}}{2\Delta t} \right),$$

$$\tilde{\theta}_0 = \frac{1}{\tilde{\alpha}} \left(-\frac{m_{n-1}}{\Delta t^2}, -\frac{m_{n-1}}{\Delta t^2} - \frac{c_{(n-1)(n-1)} + c_{n(n-1)} + c_{n(n-2)}}{2\Delta t}, -\frac{c_{n(n-1)}}{2\Delta t} \right),$$

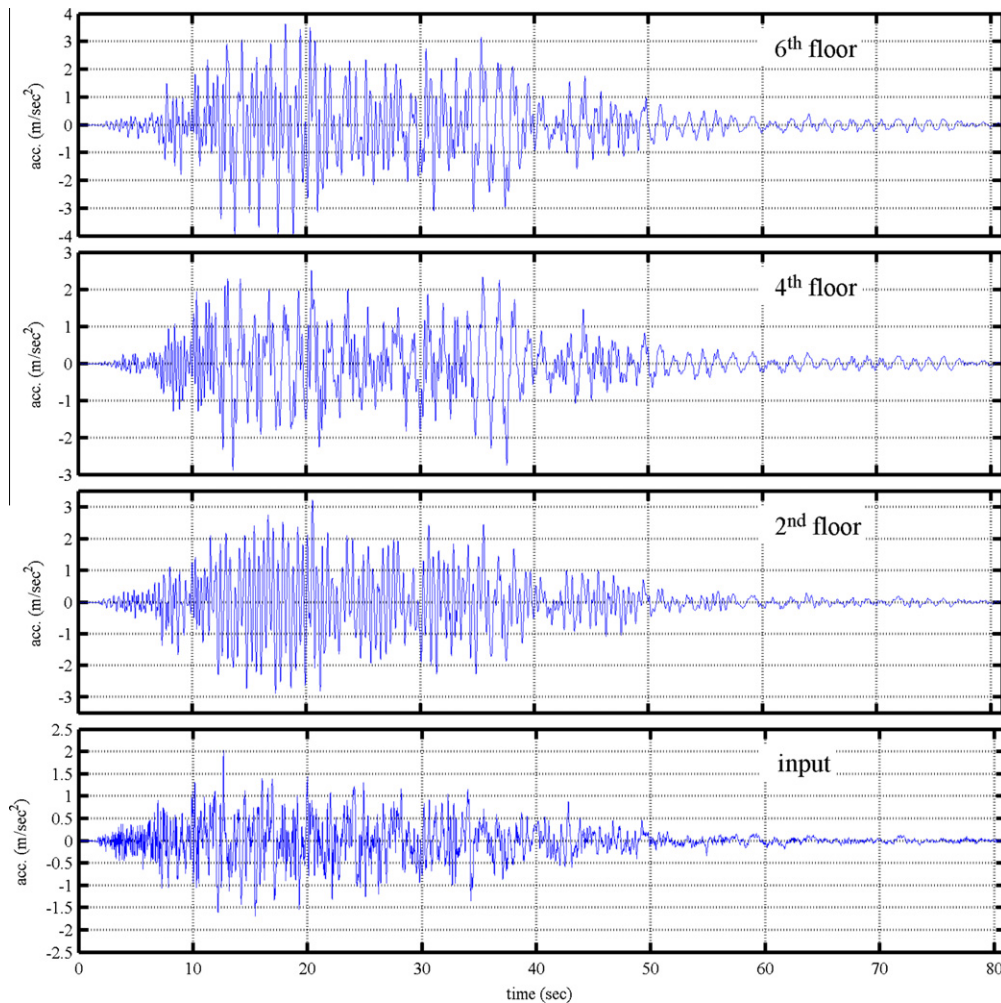


Fig. 2. Simulated earthquake responses.

$$\begin{aligned} \bar{\theta}_1 &= \frac{1}{\bar{\alpha}} \left(\frac{2m_{n-1}}{\Delta t^2}, \frac{2m_{n-1}}{\Delta t^2}, k_n \right), \\ \bar{\theta}_2 &= \frac{1}{\bar{\alpha}} \left(-\frac{m_{n-1}}{\Delta t^2}, -\frac{m_{n-1}}{\Delta t^2} + \frac{c_{(n-1)(n-1)} + c_{n(n-1)} + c_{n(n-2)}}{2\Delta t}, \frac{c_{n(n-1)}}{2\Delta t} \right), \\ \bar{\phi}_1 &= \frac{1}{\bar{\alpha}} \left[\frac{2(m_{n-1} + m_n)}{\Delta t^2} - k_{n-1} \right], \\ \bar{\phi}_2 &= -\frac{1}{\bar{\alpha}} \left[\frac{m_{n-1} + m_n}{\Delta t^2} - \frac{c_{nn} + 2c_{n(n-1)} + c_{(n-1)(n-1)}}{2\Delta t} \right], \\ \bar{\theta}_0 &= \frac{1}{\bar{\alpha}} \left(-\frac{m_n + m_{n-1}}{\Delta t^2}, -\frac{2m_{n-1}}{\Delta t^2} - \frac{c_{nn} + 2c_{n(n-1)} + c_{(n-1)(n-1)} + c_{(n-1)(n-2)}}{2\Delta t}, \right. \\ &\quad \left. -\frac{c_{n(n-1)} + c_{nn}}{2\Delta t} - \frac{m_n}{\Delta t^2} \right), \\ \bar{\theta}_1 &= \frac{1}{\bar{\alpha}} \left(\frac{2(m_n + m_{n-1})}{\Delta t^2}, \frac{4m_{n-1}}{\Delta t^2}, \frac{2m_n}{\Delta t^2} \right), \\ \bar{\theta}_2 &= \frac{1}{\bar{\alpha}} \left(-\frac{m_n + m_{n-1}}{\Delta t^2}, -\frac{2m_{n-1}}{\Delta t^2} + \frac{c_{nn} + 2c_{n(n-1)} + c_{(n-1)(n-1)} + c_{(n-1)(n-2)}}{2\Delta t}, \right. \\ &\quad \left. \frac{c_{n(n-1)} + c_{nn}}{2\Delta t} - \frac{m_n}{\Delta t^2} \right), \\ \bar{\mathbf{y}}(t-j) &= (a_g(t-j), \ddot{x}_{n-2}(t-j), \ddot{x}_n^r(t-j))^T, \\ \hat{\alpha} &= \frac{m_{n-1}}{\Delta t^2} + \frac{c_{(n-1)(n-1)} + c_{n(n-1)}}{2\Delta t}, \\ \bar{\alpha} &= \frac{m_{n-1} + m_n}{\Delta t^2} + \frac{c_{nn} + 2c_{n(n-1)} + c_{(n-1)(n-1)}}{2\Delta t}. \end{aligned}$$

Eqs. (14) and (15) are ARX models with the same form but different coefficients. Hence, when \ddot{x}_{n-1}^r is used as an output and a_g, \ddot{x}_{n-2} and \ddot{x}_n^r are used as inputs of an ARX model, if the differential equation

that is equivalent to the ARX model cannot be determined, then the natural frequency that is evaluated from the established ARX model is useless. Unfortunately, establishing a rule to determine the differential equation that correctly corresponds to an established ARX model is generally impossible because twice differentiating any linear combinations of Eq. (12b) with $j = n - 1$ and Eq. (13) with respect to t yield the ARX models that have the same form as that given in Eqs. (14) and (15). The conclusion is the same when free vibration responses are utilized to establish an ARX model.

To overcome the aforementioned difficulty in identifying the natural frequency of the $(n - 1)$ th sub-structure, a multiple-input/multiple-output (MIMO) ARX model is firstly constructed with \ddot{x}_n and \ddot{x}_{n-1} as outputs and a_g and \ddot{x}_{n-2} as inputs. The theoretical natural frequencies that are identified from such an MIMO ARX model are denoted ω_1 and ω_2 (rad/s). The established MIMO ARX model corresponds to the following equations of motion for the n th and $(n - 1)$ th DOFs,

$$\begin{aligned} \begin{bmatrix} m_n & 0 \\ 0 & m_{n-1} \end{bmatrix} \begin{bmatrix} \ddot{x}_n \\ \ddot{x}_{n-1} \end{bmatrix} + \begin{bmatrix} c_{nn} & c_{n(n-1)} \\ c_{n(n-1)} & c_{(n-1)(n-1)} \end{bmatrix} \begin{bmatrix} \dot{x}_n \\ \dot{x}_{n-1} \end{bmatrix} \\ + \begin{bmatrix} k_n & -k_n \\ -k_n & k_n + k_{n-1} \end{bmatrix} \begin{bmatrix} x_n \\ x_{n-1} \end{bmatrix} = \begin{bmatrix} -m_n a_g \\ -m_{n-1} a_g \end{bmatrix} \\ + \begin{bmatrix} 0 \\ c_{(n-1)(n-2)} \ddot{x}_{n-2} + k_{n-1} x_{n-2} \end{bmatrix} \end{aligned} \quad (16)$$

The following relation

$$\omega_1 \omega_2 = \sqrt{\frac{k_{n-1} k_n}{m_{n-1} m_n}} \quad (17)$$

is easy to find from Eq. (16). Notably, $\sqrt{k_n/m_n}$ (rad/s) is the theoretical natural frequency determined from Eq. (12a) and can be identified from the MISO ARX model established with \ddot{x}_n^r as an output and a_g and \ddot{x}_{n-1} as inputs. Consequently, $\sqrt{k_{n-1}/m_{n-1}}$ (rad/s), which

Table 2
Identified modal parameters of full structures.

No. of damage case	Modal parameters	Mode					
		1	2	3	4	5	6
1 (-10% k_1)	\bar{f}_n (Hz)	0.755(0.755)	2.23(2.23)	3.58(3.58)	4.73(4.73)	5.62(5.62)	6.18(6.18)
	ξ (%)	5.51(5.51)	2.49(2.49)	2.24(2.24)	2.33(2.33)	2.47(2.47)	2.58(2.58)
	MAC	1.00(1.00)	1.00(1.00)	1.00(1.00)	1.00(1.00)	1.00(1.00)	1.00(1.00)
2 (-20% k_1)	\bar{f}_n (Hz)	0.740(0.740)	2.19(2.19)	3.54(3.54)	4.70(4.70)	5.60(5.60)	6.17(6.17)
	ξ (%)	5.61(5.61)	2.51(2.51)	2.24(2.24)	2.32(2.32)	2.47(2.47)	2.58(2.58)
	MAC	1.00(1.00)	1.00(1.00)	0.99(0.99)	0.99(0.99)	1.00(1.00)	1.00(1.00)
3 (-10% k_5)	\bar{f}_n (Hz)	0.765(0.765)	2.22(2.22)	3.59(3.59)	4.76(4.76)	5.55(5.55)	6.13(6.13)
	ξ (%)	5.44(5.44)	2.49(2.49)	2.24(2.24)	2.33(2.33)	2.46(2.46)	2.57(2.57)
	MAC	1.00(1.00)	1.00(1.00)	1.00(1.00)	1.00(1.00)	0.98(0.98)	0.98(0.98)
4 (-20% k_5)	\bar{f}_n (Hz)	0.761(0.761)	2.17(2.17)	3.56(3.56)	4.75(4.75)	5.46(5.46)	6.09(6.09)
	ξ (%)	5.47(5.47)	2.51(2.51)	2.24(2.24)	2.33(2.33)	2.44(2.44)	2.57(2.57)
	MAC	1.00(1.00)	1.00(1.00)	0.99(0.99)	1.00(1.00)	0.94(0.94)	0.95(0.95)
5 (-10% k_1 and k_4)	\bar{f}_n (Hz)	0.749(0.749)	2.20(2.20)	3.57(3.57)	4.66(4.66)	5.61(5.61)	6.09(6.09)
	ξ (%)	5.55(5.55)	2.50(2.50)	2.24(2.24)	2.32(2.32)	2.47(2.47)	2.57(2.57)
	MAC	1.00(1.00)	1.00(1.00)	1.00(1.00)	1.00(1.00)	1.00(1.00)	1.00(1.00)
6 (-10% k_1 and -20% k_4)	\bar{f}_n (Hz)	0.743(0.743)	2.17(2.17)	3.55(3.55)	4.58(4.58)	5.61(5.61)	6.00(6.00)
	ξ (%)	5.59(5.59)	2.52(2.52)	2.24(2.24)	2.31(2.31)	2.47(2.47)	2.55(2.55)
	MAC	1.00(1.00)	1.00(1.00)	1.00(1.00)	0.98(0.98)	0.99(0.99)	0.98(0.98)
7 (-10% k_4 and k_5)	\bar{f}_n (Hz)	0.759(0.759)	2.20(2.20)	3.57(3.57)	4.69(4.69)	5.54(5.54)	6.04(6.04)
	ξ (%)	5.48(5.48)	2.50(2.50)	2.24(2.24)	2.32(2.32)	2.46(2.46)	2.56(2.56)
	MAC	1.00(1.00)	1.00(1.00)	1.00(1.00)	1.00(1.00)	0.96(0.96)	0.96(0.96)
8 (-20% k_4 and -10% k_5)	\bar{f}_n (Hz)	0.752(0.752)	2.17(2.17)	3.56(3.56)	4.62(4.62)	5.52(5.52)	5.97(5.97)
	ξ (%)	5.53(5.53)	2.52(2.52)	2.24(2.24)	2.31(2.31)	2.46(2.46)	2.54(2.54)
	MAC	1.00(1.00)	1.00(1.00)	0.99(0.99)	0.98(0.98)	0.93(0.93)	0.92(0.92)
Intact	\bar{f}_n (Hz)	0.767(0.767)	2.26(2.26)	3.62(3.62)	4.77(4.77)	5.64(5.64)	6.18(6.18)
	ξ (%)	5.43(5.43)	2.47(2.47)	2.24(2.24)	2.33(2.33)	2.48(2.48)	2.59(2.59)

Table 3
Frequencies and damping ratios of sub-structures identified from simulated earthquake responses without noise.

No. of damage case	Modal parameters	Sub-structure					
		1	2	3	4	5	6
1 (−10% k_1)	\bar{f}_n (Hz)	3.02(3.02)	3.18(3.18)	3.18(3.18)	3.18(3.18)	3.18(3.18)	3.18(3.18)
	ξ (%)	2.27(2.27)	2.25(2.25)	2.25(2.25)	2.25(2.25)	/ (2.25)	2.25(2.25)
2 (−20% k_1)	\bar{f}_n (Hz)	2.85(2.85)	3.18(3.18)	3.18(3.18)	3.18(3.18)	3.18(3.18)	3.18(3.18)
	ξ (%)	2.29(2.29)	2.25(2.25)	2.25(2.25)	2.25(2.25)	/ (2.25)	2.25(2.25)
3 (−10% k_5)	\bar{f}_n (Hz)	3.18(3.18)	3.18(3.18)	3.18(3.18)	3.18(3.18)	3.02(3.02)	3.18(3.18)
	ξ (%)	2.25(2.25)	2.25(2.25)	2.25(2.25)	2.25(2.25)	/ (2.27)	2.25(2.25)
4 (−20% k_5)	\bar{f}_n (Hz)	3.18(3.18)	3.18(3.18)	3.18(3.18)	3.18(3.18)	2.85(2.85)	3.18(3.18)
	ξ (%)	2.25(2.25)	2.25(2.25)	2.25(2.25)	2.25(2.25)	/ (2.29)	2.25(2.25)
5 (−10% k_1 and k_4)	\bar{f}_n (Hz)	3.02(3.02)	3.18(3.18)	3.18(3.18)	3.02(3.02)	3.18(3.18)	3.18(3.18)
	ξ (%)	2.27(2.27)	2.25(2.25)	2.25(2.25)	2.27(2.27)	/ (2.25)	2.25(2.25)
6 (−10% k_1 and −20% k_4)	\bar{f}_n (Hz)	3.02(3.02)	3.18(3.18)	3.18(3.18)	2.85(2.85)	3.18(3.18)	3.18(3.18)
	ξ (%)	2.27(2.27)	2.25(2.25)	2.25(2.25)	2.29(2.29)	/ (2.25)	2.25(2.25)
7 (−10% k_4 and k_5)	\bar{f}_n (Hz)	3.18(3.18)	3.18(3.18)	3.18(3.18)	3.02(3.02)	3.02(3.02)	3.18(3.18)
	ξ (%)	2.25(2.25)	2.25(2.25)	2.25(2.25)	2.27(2.27)	/ (2.27)	2.25(2.25)
8 (−20% k_4 and −10% k_5)	\bar{f}_n (Hz)	3.18(3.18)	3.18(3.18)	3.18(3.18)	2.85(2.85)	3.02(3.02)	3.18(3.18)
	ξ (%)	2.25(2.25)	2.25(2.25)	2.25(2.25)	2.29(2.29)	/ (2.27)	2.25(2.25)
Intact	\bar{f}_n (Hz)	3.18(3.18)	3.18(3.18)	3.18(3.18)	3.18(3.18)	3.18(3.18)	3.18(3.18)
	ξ (%)	2.25(2.25)	2.25(2.25)	2.25(2.25)	2.25(2.25)	/ (2.25)	2.25(2.25)

Note: Those bold-face values are the sub-structural frequencies and damping ratios corresponding to the stories whose stiffness is changed. “/” indicates data not available.

Table 4
COMAC values and normalized results from FRFCM.

No. of damage case	Method	Floor					
		1	2	3	4	5	6
1 (−10% k_1)	COMAC	1.00	1.00	1.00	1.00	1.00	1.00
	FRFCM	1.00	0.53	0.68	0.54	0.50	0.25
2 (−20% k_1)	COMAC	0.99	0.99	0.99	1.00	1.00	1.00
	FRFCM	1.00	0.52	0.67	0.52	0.49	0.24
3 (−10% k_5)	COMAC	1.00	0.99	0.99	0.99	0.99	1.00
	FRFCM	0.91	0.59	1.00	0.89	0.83	0.41
4 (−20% k_5)	COMAC	0.99	0.98	0.97	0.98	0.97	0.99
	FRFCM	0.92	0.60	1.00	0.88	0.84	0.42
5 (−10% k_1 and k_4)	COMAC	1.00	0.99	1.00	1.00	1.00	1.00
	FRFCM	1.00	0.49	0.76	0.73	0.74	0.37
6 (−10% k_1 and −20% k_4)	COMAC	0.98	0.98	1.00	0.99	0.99	1.00
	FRFCM	1.00	0.46	0.83	0.88	0.91	0.46
7 (−10% k_4 and k_5)	COMAC	0.98	0.97	0.98	0.99	0.99	1.00
	FRFCM	0.89	0.46	0.87	0.96	1.00	0.50
8 (−20% k_4 and −10% k_5)	COMAC	0.96	0.94	0.97	0.97	0.98	1.00
	FRFCM	0.82	0.40	0.81	0.95	1.00	0.50

is the theoretical natural frequency for the sub-structure described by Eq. (12b) with $j = n - 1$, can be obtained using Eq. (17).

As a brief summary, the procedure of locating damaged storeys from the earthquake responses of a shear building is as follows:

- (1) Establish an MISO ARX model from \ddot{x}_n^r , a_g and \ddot{x}_{n-1} to identify natural frequency, $\sqrt{k_n/m_n}$, and damping ratio, $c_{nn}/(2\sqrt{m_n k_n})$,
- (2) Establish MISO ARX models from \ddot{x}_j^r , a_g , \ddot{x}_{j-1} and \ddot{x}_{j+1}^r for $j=2$ to $n-2$ to identify natural frequency, $\sqrt{k_j/m_j}$, and damping ratio, $(c_{jj} + c_{(j+1)j})/(2\sqrt{m_j k_j})$,
- (3) Construct an MISO ARX model from \ddot{x}_1 , a_g and \ddot{x}_2^r to find natural frequency, $\sqrt{k_1/m_1}$, and damping ratio, $c_{11}/(2\sqrt{m_1 k_1})$,
- (4) Construct an MIMO ARX model from \ddot{x}_n , \ddot{x}_{n-1} , \ddot{x}_{n-2} , and a_g to determine $\sqrt{(k_{n-1}k_n)/(m_{n-1}m_n)}$,
- (5) Determine $\sqrt{k_{n-1}/m_{n-1}}$ from the results of steps (1) and (4),

- (6) Compare the natural frequencies of all sub-structures in the current state with those in the undamaged state to locate the storeys that may have been damaged.

When free vibration responses of a building are processed, a_g in the above procedure is eliminated. Notably, the MISO ARX models and MIMO ARX models are established and the corresponding frequencies and damping ratios are determined using the procedure given in the previous section.

4. Numerical simulation and comparisons

Numerically simulated responses of a six-storey shear building were processed to demonstrate the accuracy and effectiveness of the proposed approach in locating damaged storeys. The numerical examples incorporate most of the complications encountered in real applications, i.e., noise in the measurements of input and output and multiple damaged storeys with damage of different severity. The stiffness and mass of each floor of the shear building are $k_i = 40$ kN/m and $m_i = 0.1$ t, respectively. Rayleigh damping is assumed, and the damping matrix is expressed as $\mathbf{C} = \alpha\mathbf{M} + \beta\mathbf{K}$, where $\alpha = 0.5$ s^{−1} and $\beta = 0.001$ s. Eight cases of damage, including various degrees of single-site and dual-site damage, given in Table 1, were examined.

4.1. Simulating earthquake responses

The north-south component of the 1999 Chi-Chi earthquake, which was recorded in a free field, was used to excite the shear building. Fig. 2 displays the input excitations and the responses of the second, fourth and sixth floors. The acceleration responses of each floor and input base excitations, sampled at 250 Hz, were used to determine the modal parameters in Table 2 for the full structure under various damage conditions. Comparisons of the natural frequencies (\bar{f}_n) and damping ratios (ξ) thus obtained with the theoretical values, given in parentheses in Table 2, reveal that the identified natural frequencies and modal damping ratios are accurate to three significant figures, demonstrating the accuracy of the identification method based on the continuous wavelet transform. Values of MAC indicate a correlation between the modal

Table 5
Frequencies and damping ratios of sub-structures identified from simulated earthquake responses with 20% noise.

No. of damage case	Modal parameters	Sub-structure					
		1	2	3	4	5	6
1 (–10% k_1)	\bar{f}_n (Hz)	3.01(3.02)	3.18(3.18)	3.18(3.18)	3.16(3.18)	3.19(3.18)	3.19(3.18)
	ξ (%)	2.94(2.27)	2.69(2.25)	2.50(2.25)	2.06(2.25)	/(2.25)	2.30(2.25)
2 (–20% k_1)	\bar{f}_n (Hz)	2.84(2.85)	3.17(3.18)	3.18(3.18)	3.17(3.18)	3.18(3.18)	3.18(3.18)
	ξ (%)	2.11(2.29)	2.89(2.25)	2.58(2.25)	2.12(2.25)	/(2.25)	2.43(2.25)
3 (–10% k_5)	\bar{f}_n (Hz)	3.17(3.18)	3.17(3.18)	3.17(3.18)	3.18(3.18)	3.02(3.02)	3.19(3.18)
	ξ (%)	2.10(2.25)	2.73(2.25)	2.30(2.25)	3.04(2.25)	/(2.27)	2.29(2.25)
4 (–20% k_5)	\bar{f}_n (Hz)	3.18(3.18)	3.18(3.18)	3.17(3.18)	3.20(3.18)	2.87(2.85)	3.18(3.18)
	ξ (%)	2.04(2.25)	2.78(2.25)	2.24(2.25)	3.97(2.25)	/(2.29)	2.39(2.25)
5 (–10% k_1 and k_4)	\bar{f}_n (Hz)	3.01(3.02)	3.18(3.18)	3.18(3.18)	3.02(3.02)	3.17(3.18)	3.19(3.18)
	ξ (%)	2.02(2.27)	2.83(2.25)	2.56(2.25)	2.32(2.27)	/(2.25)	2.38(2.25)
6 (–10% k_1 and –20% k_4)	\bar{f}_n (Hz)	3.02(3.02)	3.18(3.18)	3.18(3.18)	2.85(2.85)	3.20(3.18)	3.18(3.18)
	ξ (%)	2.10(2.27)	2.85(2.25)	2.50(2.25)	2.53(2.29)	/(2.25)	2.17(2.25)
7 (–10% k_4 and k_5)	\bar{f}_n (Hz)	3.18(3.18)	3.18(3.18)	3.18(3.18)	3.01(3.02)	3.02(3.02)	3.19(3.18)
	ξ (%)	2.20(2.25)	2.79(2.25)	2.65(2.25)	2.76(2.27)	/(2.25)	2.73(2.25)
8 (–20% k_4 and –10% k_5)	\bar{f}_n (Hz)	3.18(3.18)	3.18(3.18)	3.18(3.18)	2.83(2.85)	3.02(3.02)	3.19(3.18)
	ξ (%)	2.17(2.25)	2.82(2.25)	2.68(2.25)	2.97(2.25)	/(2.25)	2.72(2.25)
Intact	\bar{f}_n (Hz)	3.17(3.18)	3.17(3.18)	3.19(3.18)	3.19(3.18)	3.19(3.18)	3.19(3.18)
	ξ (%)	2.06(2.25)	2.69(2.25)	2.62(2.25)	3.05(2.25)	/(2.25)	2.16(2.25)

Note: Those bold-face values are the sub-structural frequencies and damping ratios corresponding to the stories whose stiffness is changed. “/” indicates data not available.

shapes of the intact structure and those of the damaged structure. Damage changes the natural frequencies of structures. Severe damage as in case six causes changes in the frequencies of the second and fourth modes of up to 3.98%. However, determining from the values of MAC whether a structure is damaged or not is difficult because most of the MAC values in Table 2 exceed 0.98, and are too close to unity, except for the fifth and sixth modes in cases four, seven and eight.

Table 3 summarizes the identified natural frequencies and damping ratios of various sub-structures. In Table 3, the j th sub-structure includes the $(j - 1)$ th, j th and $(j + 1)$ th floors when j is not equal to one or six. The first sub-structure contains the first and second floors while the sixth sub-structure contains the fifth and sixth floors. The results in parentheses are exact values. The identified results and the exact values are identical to three significant figures. The damping ratio of the fifth sub-structure is not available because the identification procedure that was described in the preceding section does not give the damping ratio of the $(n - 1)$ th sub-structure. The locations of the damaged storeys are assessed by the differences between the natural frequencies of the damaged and undamaged sub-structures. The damping ratios of the sub-structures are not employed to locate the damaged storeys because the damping ratios of a real building depend on its amplitude of vibration, and the accuracy of the identified damping ratios is typically much lower than that of the identified natural frequencies, especially when responses are noisy.

Table 3 reveals that damage to a storey reduces the natural frequency of the sub-structure that includes the damaged storey. Comparisons of damage cases one and three with cases two and four, respectively, demonstrate that the changes in the frequencies of the sub-structures are proportional to the changes in the square root of the stiffness of a damaged storey. Comparing the sub-structural natural frequencies in the intact structure with those in cases five and six shows that only the natural frequencies of the first and fourth sub-structures change, whereas the natural frequencies of the other sub-structures do not change. The changes in the natural frequencies of the first and fourth sub-structures in case six are 5.03% and 10.38%, respectively. The differences between the

sub-structural natural frequencies in the damaged and undamaged states accurately reflect the changes in their stiffness. The results also indicate that the present approach accurately locates multiple storeys with various extents of damage. Comparisons of the results in Tables 2 and 3 reveal that damage causes much more significant change in the frequency of a sub-structure than in that of the full structure. Accordingly, locating the damaged storeys using the natural frequencies of the substructures is easier than doing so using the natural frequencies of a full structure.

To demonstrate further the superiority of the present approach to some of the methods in the literature, Table 4 shows the values of COMAC (coordinate modal assurance criterion) [16] and the normalized results that were obtained using the frequency response function curvature method (FRFCM) [26]. In FRFCM, the magnitude of frequency response function for the i th DOF was simply estimated by $|\ddot{X}_i|/|A_g|$, where $|\ddot{X}_i|$ and $|A_g|$ are the magnitudes of the Fourier transforms of relative acceleration responses of the i th DOF and input acceleration, respectively, and the Fourier transform is practically calculated at discrete circular frequencies using Fast Fourier transform. The absolute differences between the frequency response function curvatures of the damaged and undamaged structures at floor i were computed for the frequency range from 0 to 10 Hz, which covers all of the natural frequencies. The values of COMAC are between zero and unity. Larger values of COMAC correspond to less damage in a DOF; larger normalized values obtained by the FRFCM indicate more severe damage. Table 4 discovers that the values of COMAC and the results from FRFCM do not correctly identify the damaged storeys. Even when a storey is damaged with a 20% decrease in stiffness (as in cases two and four), the corresponding COMAC value is only slightly smaller than unity. Except for the second floor in case eight, all of the values of COMAC exceed 0.96, raising difficulty in correctly identifying the damaged storeys. In damage cases one and two, although the greatest values obtained by FRFCM are correctly at the first floor, the values for the undamaged floors are not close to zero, and most are more than 50% of the maximum results. The highest values obtained from FRFCM are at the undamaged floors in cases three and four. Comparison of the results in Tables 3 and 4 clearly reveals that the proposed procedure outperforms the frequency response function

curvature method or the use of COMAC in correctly locating the damaged storeys.

Measured responses always contain some corrupting noise. To simulate this fact, independent Gaussian white noise with a 20% variance in the noise-to-signal ratio (NSR) was randomly added to the computed acceleration responses and input base excitation. Table 5 lists the sub-structural frequencies identified from the

noisy responses and input. Again, the results in parentheses are theoretical values. The identified natural frequencies in all of the damage cases agree excellently with the theoretical values. Comparison of the identified natural frequencies in Tables 3 and 5 reveals that 20% noise does not significantly influence the accuracy of the present results. However, the noise markedly affects the accuracy of the identified damping ratio of each sub-structure.

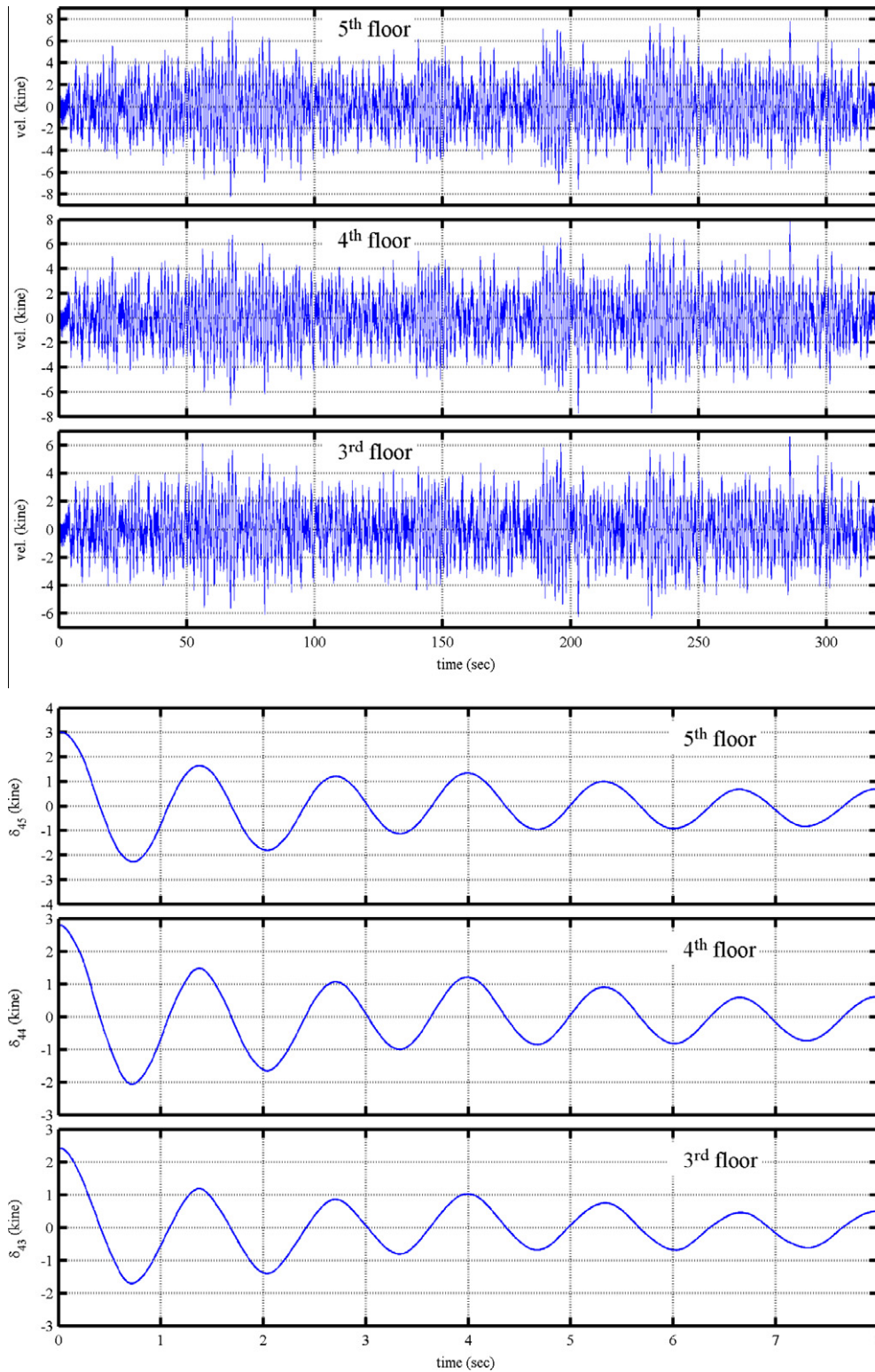


Fig. 3. Simulated ambient vibration responses and corresponding Randomdec signatures.

Table 6
Frequencies and damping ratios of sub-structures identified from simulated ambient vibration responses with 20% noise.

No. of damage case	Modal parameters	Sub-structure					
		1	2	3	4	5	6
1 (−10% k_1)	\bar{f}_n (Hz)	3.02(3.02)	3.18(3.18)	3.18(3.18)	3.17(3.18)	3.18(3.18)	3.18(3.18)
	ξ (%)	2.22(2.27)	2.57(2.25)	2.33(2.25)	2.24(2.25)	/ (2.25)	2.22(2.25)
2 (−20% k_1)	\bar{f}_n (Hz)	2.85(2.85)	3.18(3.18)	3.17(3.18)	3.17(3.18)	3.18(3.18)	3.18(3.18)
	ξ (%)	2.26(2.29)	2.59(2.25)	2.32(2.25)	2.07(2.25)	/ (2.25)	2.20(2.25)
3 (−10% k_5)	\bar{f}_n (Hz)	3.18(3.18)	3.18(3.18)	3.17(3.18)	3.17(3.18)	3.02(3.02)	3.18(3.18)
	ξ (%)	2.21(2.25)	2.51(2.25)	2.30(2.25)	2.11(2.25)	/ (2.27)	2.23(2.25)
4 (−20% k_5)	\bar{f}_n (Hz)	3.18(3.18)	3.18(3.18)	3.17(3.18)	3.18(3.18)	2.85(2.85)	3.18(3.18)
	ξ (%)	2.21(2.25)	2.39(2.25)	2.11(2.25)	2.06(2.25)	/ (2.29)	2.25(2.25)
5 (−10% k_1 and k_4)	\bar{f}_n (Hz)	3.02(3.02)	3.18(3.18)	3.17(3.18)	3.01(3.02)	3.18(3.18)	3.18(3.18)
	ξ (%)	2.22(2.27)	2.47(2.25)	2.20(2.25)	2.08(2.27)	/ (2.25)	2.21(2.25)
6 (−10% k_1 and −20% k_4)	\bar{f}_n (Hz)	3.02(3.02)	3.18(3.18)	3.17(3.18)	2.84(2.85)	3.18(3.18)	3.18(3.18)
	ξ (%)	2.22(2.27)	2.53(2.25)	2.02(2.25)	2.14(2.29)	/ (2.25)	2.25(2.25)
7 (−10% k_4 and k_5)	\bar{f}_n (Hz)	3.18(3.18)	3.18(3.18)	3.17(3.18)	3.01(3.02)	3.02(3.02)	3.18(3.18)
	ξ (%)	2.22(2.25)	2.49(2.25)	2.11(2.25)	2.00(2.27)	/ (2.27)	2.22(2.25)
8 (−20% k_4 and −10% k_5)	\bar{f}_n (Hz)	3.18(3.18)	3.18(3.18)	3.18(3.18)	2.84(2.85)	3.02(3.02)	3.18(3.18)
	ξ (%)	2.20(2.25)	2.36(2.25)	2.45(2.25)	2.02(2.29)	/ (2.27)	2.21(2.25)
Intact	\bar{f}_n (Hz)	3.18(3.18)	3.18(3.18)	3.17(3.18)	3.17(3.18)	3.18(3.18)	3.18(3.18)
	ξ (%)	2.20(2.25)	2.59(2.25)	2.31(2.25)	2.10(2.25)	/ (2.25)	2.28(2.25)

Note: Those bold-face values are the sub-structural frequencies and damping ratios corresponding to the stories whose stiffness is changed. “/” indicates data not available.

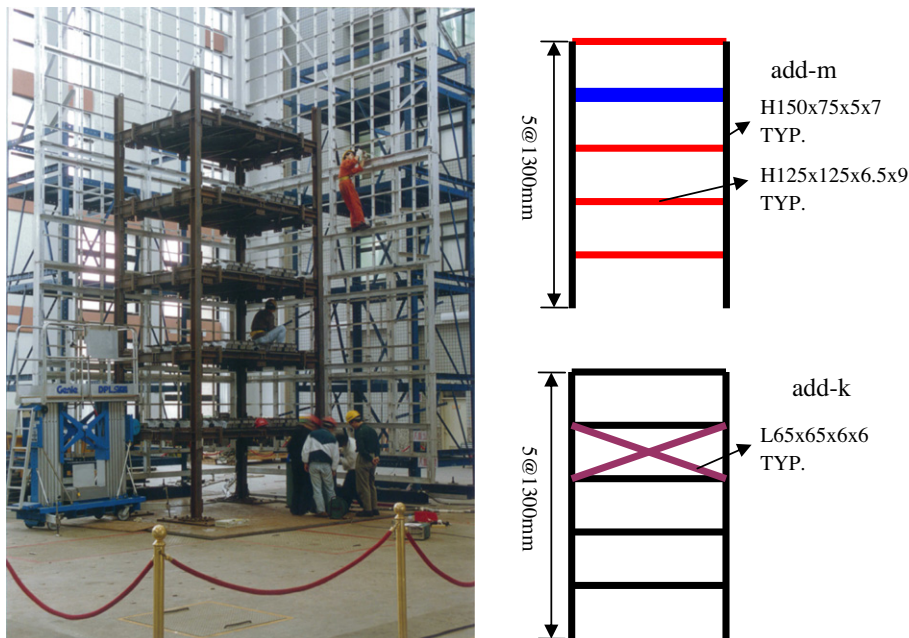


Fig. 4. A photo of frame “std” and simple sketch of frames “add-m” and “add-k”.

4.2. Simulating ambient vibration responses

Ambient vibration tests are popular *in situ* tests for monitoring the dynamic behaviors of a structure. Unlike a system for monitoring responses to earthquake, an ambient vibration measuring system, especially a wireless system, is portable, and so can be easily used to measure the dynamic responses of a structure anytime and at any location. Therefore, measuring the ambient vibration responses of any sub-structure of a building is an easy task. To demonstrate the applicability of the proposed procedure to processing the ambient vibration responses of a building for locating possibly damaged storeys, ambient vibration responses of the six-storey shear building, considered in the previous section, are simulated

under an external force vector $\mathbf{f} = (1, 1, 1, 1, 1, 1)^T a$, where a is a white noise process with zero mean. Five minutes of ambient vibration responses for all six DOFs were processed and sampled at 200 Hz.

Since measured responses are normally contaminated by noise, independent Gaussian white noise with a 20% variance in the noise-to-signal ratio was randomly added to the computed velocity responses. Processing the velocity responses without noise using the random decrement technique [40] yielded Randomdec signatures, which are equivalent to the free decay responses of the structure [41]. Fig. 3 depicts parts of the noisy ambient vibration responses and the corresponding Randomdec signatures. Natural frequencies and damping ratios of sub-structures were obtained

by employing the procedure that is presented in Section 3 to analyze the Randomdec signatures. For example, to estimate the natural frequency and damping ratio of the j th sub-structure, which includes the $(j - 1)$ th, j th and $(j + 1)$ th DOFs, the random decrement technique was applied to the noisy velocity responses of these DOFs to obtain the auto-Randomdec signature and cross-Randomdec signatures with respect to the responses of the j th DOF. Let $\delta_{jj}(t)$ be the obtained auto-Randomdec signature of the responses of DOF j , while $\delta_{j(j-1)}(t)$ and $\delta_{j(j+1)}(t)$ represent the

cross-Randomdec signatures of the responses of DOFs $(j - 1)$ and $(j + 1)$, respectively. Then, an MISO ARX model can be constructed with $\tilde{\delta}_j^r(t)$ as output and $\tilde{\delta}_{j+1}^r(t)$ and $\delta_{j(j-1)}(t)$ as inputs, where $\tilde{\delta}_j^r(t) = \delta_{jj}(t) - \delta_{j(j-1)}(t)$ and $\tilde{\delta}_{j+1}^r(t) = \delta_{j(j+1)}(t) - \delta_{jj}(t)$. Then, the natural frequency and damping ratio of the j th sub-structure are estimated from the established MISO ARX model.

Table 6 summarizes the natural frequencies and damping ratios that were obtained from the simulated ambient vibration responses with noise (NSR = 20%). The exact values are given in

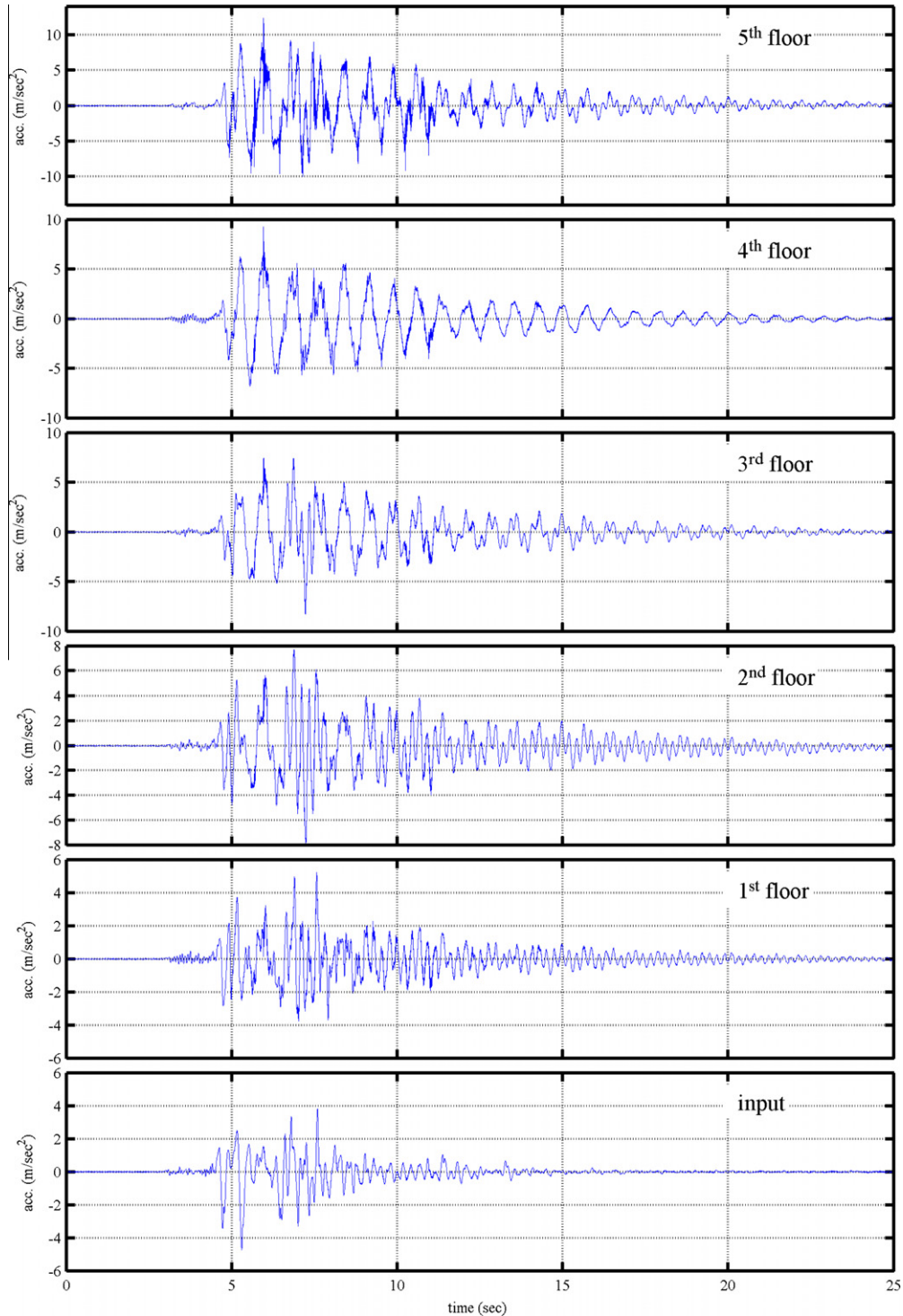


Fig. 5. The acceleration responses of frame “std” in the long-span direction subjected to 60% Kobe earthquake.

Table 7
Identified modal parameters of steel frames.

Frame	Modal parameters	Mode				
		1	2	3	4	5
std	\bar{f}_n (Hz)	1.40	4.53	8.23	12.39	15.98
	ξ (%)	1.59	0.18	0.20	0.15	0.18
add-k	\bar{f}_n (Hz)	1.52	5.94	8.23	13.99	18.37
	ξ (%)	1.81	0.20	0.16	0.14	1.66
	MAC	0.99	0.91	1.00	0.65	0.80
add-m	\bar{f}_n (Hz)	1.34	4.52	8.06	11.93	15.73
	ξ (%)	1.42	0.19	0.25	0.17	0.29
	MAC	1.00	1.00	0.99	0.98	0.99
std-yield	\bar{f}_n (Hz)	1.35	4.44	8.08	12.18	15.48
	ξ (%)	4.31	1.08	1.40	0.93	1.48
	MAC	1.00	1.00	0.99	0.99	0.98

Table 8
Identified sub-structural frequencies and damping ratios of five-storey steel frames.

Frame	Modal parameters	Sub-structure				
		1	2	3	4	5
std	\bar{f}_n (Hz)	7.01	5.30	5.50	6.27	5.08
	ξ (%)	0.20	0.12	0.87	/	0.45
add-k	\bar{f}_n (Hz)	7.14	5.73	6.19	12.98	5.78
	ξ (%)	0.10	0.55	2.91	/	0.28
add-m	\bar{f}_n (Hz)	7.03	5.26	5.49	5.60	5.07
	ξ (%)	0.21	0.11	0.71	/	0.47
std-yield	\bar{f}_n (Hz)	6.40	5.26	5.48	6.29	5.06
	ξ (%)	0.65	0.74	2.74	/	2.06

Note: “/” denotes data unavailable.

parentheses. The identified natural frequencies of the sub-structures agree excellently with the exact values with a difference of less than 0.3%. The accuracy of the determined damping ratios is not as high as that of the determined natural frequencies. The damaged storeys in the various damage cases are easily and accurately identified by comparing the sub-structural natural frequencies of the damaged structures with those of the intact structure.

5. Application to steel frames in shaking table tests

Shaking table tests are often employed in laboratories to examine the behaviors of structures in an earthquake. To generate a set of earthquake response data for benchmark models of five-storey steel structures, NCREE (National Center for Research on Earthquake Engineering) conducted a series of shaking table tests on three steel frames, which were 3 m long, 2 m wide and 6.5 m high [42] (Fig. 4). These three frames are denoted “std”, “add-m” and “add-k”. Frame “add-k” is identical to “std” except that stiffening braces were installed in its fourth storey, while frame “add-m” differs from “std” only in that its fourth storey is 25% heavier. In the shaking table tests two accelerometers were installed in the long-span direction at the two edges of each floor, respectively. The average responses of the measured acceleration data at the two edges were used in the following analyses.

The frames were subjected to base excitation by the Kobe earthquake with various reduction levels. Frame “add-m” and “add-k” were subjected to 10% and 8% Kobe earthquake, respectively. Frame “std” was subjected to 8% and 60% Kobe earthquake. Fig. 5 plots the acceleration responses of the floors in the long-span direction for frame “std”, subjected to 60% Kobe earthquake. Notably, such an intense earthquake caused the columns in the first storey to yield. For convenience, the frame that responded nonlinearly

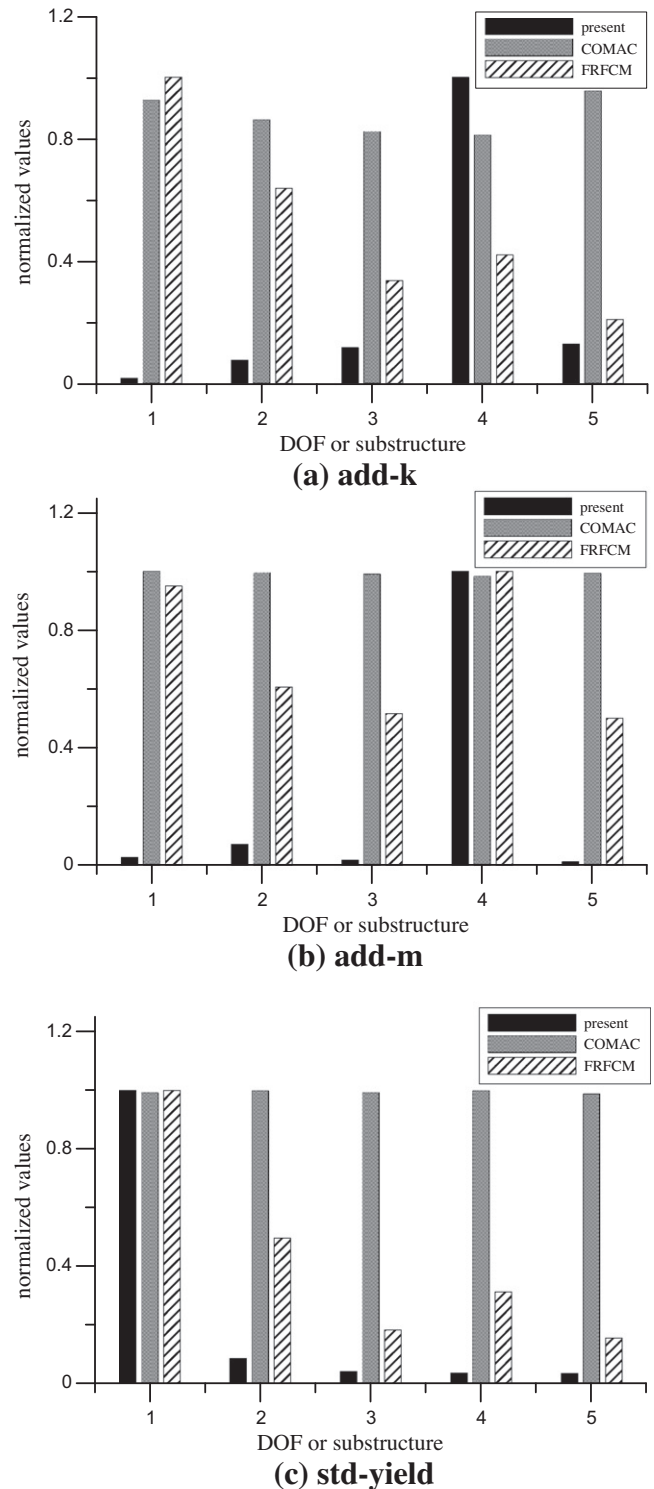


Fig. 6. Comparison of the results obtained from different methods.

is denoted “std-yield” in the following analyses. The acceleration responses of all floors at $t = 5-10$ s were used in evaluating modal parameters for each frame. The responses were sampled at 200 Hz.

The acceleration responses of each floor and the base excitations in the long-span direction were adopted to determine the modal parameters for the full frames by employing the continuous wavelet transform. Table 7 presents the results thus obtained. The MAC values for “add-m”, “add-k” and “std-yield” indicate the correlation between the modal shapes of these frames and the modal shapes of frame “std”. The natural frequencies of “add-k”, “add-m”

and “std-yield” differ significantly from those of “std”. As expected, frame “add-k” has higher natural frequencies than frame “std”, whereas frame “add-m” has lower natural frequencies. The MAC values for “add-m” and “std-yield” all exceed 0.98 and do not clearly reveal the differences in the modal shapes among the frames.

These steel frames are not shear buildings. However, a shear building model is adopted to fit the responses of a steel frame in shaking table tests and to find the sub-structural natural frequencies of the frame in order to explore the possible application of the proposed method to a real building. Table 8 lists the identified sub-structural frequencies for “std”, “add-m”, “add-k” and “std-yield”. Based on the design data of frame “std”, the stiffness and mass of each storey are uniform. Hence, under the assumption that the structure is a shear building, all sub-structures were expected to have the same natural frequencies. In fact, the identified frequencies of the sub-structures varied, perhaps because the dynamic behaviors of the steel frame differ considerably from those of a shear building. The use of a shear building model to fit the responses of the frame is responsible for the unexpected results. Another cause is that the construction details, such as the welding of a beam to a column, may not be consistent across all floors.

Comparing the sub-structural frequencies of frame “add-m” with those of frame “std” reveals that the main difference occurs in the fourth sub-structure. The differences in the other sub-structures are relatively minor. This finding is expected because frame “add-m” was designed to differ from “std” only in the mass of the fourth storey.

A comparison of the sub-structural frequencies of frames “add-k” and “std” discloses that the largest difference in frequency is at the fourth sub-structure, indicating that these two frames differ greatly in their fourth storeys. Significant frequency differences in the other sub-structures may be caused by the difference between the dynamic behaviors of the frames and those of the shear building models assumed herein.

The differences between the sub-structural frequencies for “std-yield” and “std” are as expected: only the first sub-structure exhibits a considerable difference and other sub-structures exhibit only slight differences. In real buildings, damage frequently occurs to the first storey under a large earthquake because the first storey is subjected to larger storey shear forces than the other storeys. The results for “std-yield” and “std” indicate that the proposed approach is highly applicable to locate possible damage in the first storey of a real building, even when the building may be very different from a shear building.

Fig. 6 compares the results obtained using the various methods. The frame “std” is treated as a reference structure. Since the COMAC values are always between zero and unity, the maximum values of the results from FRFCM were normalized to unity for comparison. The frequency response functions that are required in FRFCM were estimated by processing the acceleration responses at $t = 5–15$ s (Fig. 5). The results denoted by “present” in Fig. 6 are normalized relative changes in sub-structural frequencies. Fig. 6 clearly demonstrates that the proposed approach is superior to COMAC and FRFCM in identifying the storey whose properties differ from those of the corresponding storey in the reference structure. The success of the proposed procedure, as revealed in capturing the differences in properties of experimental frames, demonstrates the practical applicability of this procedure to a real building with symmetry.

6. Concluding remarks

The work developed a simple and efficient approach for identifying damaged storeys in a shear building, based on the fact that damage to a storey reduces the natural frequency of the

sub-structure that includes the damaged storey. Sub-structural natural frequencies are directly determined from ARX models that are established from the acceleration or velocity responses of corresponding sub-structures using the continuous wavelet transform. Comparing the natural frequencies of sub-structures in the current state with those in the undamaged state enables damaged storeys to be accurately located.

The proposed approach was demonstrated on a six-storey shear building under earthquake excitation and ambient vibration. A shear building with various extents of single-site or dual-site damage was considered. The proposed approach was validated by successfully identifying damaged storeys by processing numerically simulated responses, even when the responses and input excitations were contaminated by noise with a 20% variance of the noise-to-signal ratio. More severe damage to a storey yields a greater decrease in the identified natural frequency of the sub-structure that includes the damaged storey. Comparing the results obtained by the proposed approach with COMAC values and the results obtained using a frequency response curvature function method revealed that the present approach is substantially superior to these two methods in identifying damaged storeys.

The measured responses of three five-storey steel frames, which are not shear buildings and are 3 m long, 2 m wide and 6.5 m high, in shaking table tests were analyzed to demonstrate the applicability of the proposed approach in processing real measured data. The present method accurately identified the fact that the three frames had different mass or stiffness in the fourth storey, and that the first storey of one frame was damaged under a large earthquake. The success of the proposed approach when applied to the experimental responses demonstrates its practical applicability to a real symmetrical building.

Acknowledgements

The authors would like to thank the National Science Council of the Republic of China, Taiwan, for financially supporting this research under Contract No. NSC 97-2221-E-009-075-MY3. The appreciation is also extended to the National Center for Research on Earthquake Engineering for providing shaking table test data.

References

- [1] Natke HG. Updating computational models in the frequency domain based on measured data: a survey. *Probab Eng Mech* 1988;3(1):28–35.
- [2] Imregun M, Visser WJ. A review of model updating techniques. *Shock Vib Dig* 1991;23:9–20.
- [3] Mottershead JE, Friswell MI. Model updating in structural dynamics. *J Sound Vib* 1993;167(2):347–75.
- [4] Salawu OS. Detection of structural damage through changes in frequency: a review. *Eng Struct* 1997;19(9):718–23.
- [5] Doebling SW, Farrar CR, Prime MB. A summary review of vibration-based damage identification methods. *Shock Vib Dig* 1998;30(2):91–105.
- [6] Farrar CR, Doebling SW, Nix DA. Vibration-based structural damage identification. *Philosophical Transactions of the Royal Society. Math Phys Eng Sci* 2001;359(1778):131–50.
- [7] Chang PC, Flatau A, Liu SC. Review paper: health monitoring of civil infrastructure. *Struct Health Monit, Int J* 2003;2(3):257–67.
- [8] Brownjohn JMW. Structural health monitoring of civil infrastructure. *Philosophical Transactions of the Royal Society. Math Phys Eng Sci* 2007;365(1851):589–622.
- [9] Cawley P, Adams RD. The location of defects in structures from measurements of natural frequencies. *J Strain Anal* 1979;14(2):49–57.
- [10] Hearn G, Tesla RB. Modal analysis for damage detection in structures. *J Struct Eng, ASCE* 1991;117(10):2063–3042.
- [11] Friswell MI, Penny JET, Wilson DAL. Using vibration data and statistical measures to locate damage in structures. *Int J Anal Exp Modal Anal* 1994;9(4):239–54.
- [12] Messina A, Williams EJ, Contursi T. Structural damage detection by a sensitivity and statistical-based method. *J Sound Vib* 1998;216(5):791–808.
- [13] Zapico JL, González MP. Damage assessment using neural networks. *Mech Syst Signal Process* 2003;17(1):119–25.

- [14] Allemang RJ, Brown DL. A correlation coefficient for modal vector analysis. In: Proceedings of the first international modal analysis conference, Bethel, Connecticut; 1983. p. 110–6.
- [15] Baghiee N, Reza Esfahani M, Moslem K. Studies on damage and FRP strengthening of reinforced concrete beams by vibration monitoring. Eng Struct 2009;31(4):875–93.
- [16] Lieven NAJ, Ewins DJ. Spatial correlation of mode shapes, the coordinate modal assurance criterion (COMAC). In: Proceedings of the 6th international modal analysis conference, Kissimmee, Florida; 1988. p. 690–5.
- [17] Ndambi JM, Vantomme J, Harri K. Damage assessment in reinforced concrete beams using eigenfrequencies and mode shape derivatives. Eng Struct 2002;24(4):501–15.
- [18] Chen JC, Garba JA. On-orbit damage assessment for large space structures. AIAA J 1988;26(9):1119–26.
- [19] Stubbs N, Kim JT. Damage localization in structures without baseline modal parameters. AIAA J 1996;34(8):1644–9.
- [20] Hu H, Wang BT, Lee CH, Su JS. Damage detection of surface cracks in composite laminates using modal analysis and strain energy method. Compos Struct 2006;74(4):399–405.
- [21] Choi FC, Li J, Samali B, Crews K. Application of the modified damage index method to timber beams. Eng Struct 2003;30(4):1124–45.
- [22] Law SS, Shi ZY, Zhang LM. Structural damage detection from incomplete and noisy modal test data. J Eng Mech, ASCE 1998;124(11):1280–8.
- [23] Shi ZY, Law SS, Zhang LM. Structural damage location from modal strain energy change. J Sound Vib 1998;218(5):825–44.
- [24] Kim JT, Ryu YS, Cho HM, Stubbs N. Damage identification in beam-type structures: frequency-based method vs mode-shape-based method. Eng Struct 2003;25(1):57–67.
- [25] Pandey AK, Biswas M, Samman MM. Damage detection from changes in curvature mode shapes. J Sound Vib 1991;145(2):321–32.
- [26] Sampaio RPC, Maia NMM, Silva JMM. Damage detection using the frequency-response-function curvature method. J Sound Vib 1999;226(5):1029–42.
- [27] Lin CS. Location of modeling errors using modal test data. AIAA J 1990;28(9):1650–4.
- [28] Pandey AK, Biswas M. Damage detection in structures using changes in flexibility. J Sound Vib 1994;169(1):3–17.
- [29] Patjawit A, Knaok-Nukulchai W. Health monitoring of highway bridges based on a global flexibility index. Eng Struct 2005;27(9):1385–91.
- [30] Koh CG, See LM, Balendra T. Estimation of structural parameters in the time domain: a substructure approach. Earthquake Eng Struct Dynam 1991;20(8):787–801.
- [31] Koh CG, Hong B, Liaw CY. Substructural and progressive structural identification methods. Eng Struct 2003;25(12):1551–63.
- [32] Zhao Q, Sawada T, Hirao K, Nariyuki Y. Localized identification of MDOF structures in the frequency domain. Earthquake Eng Struct Dynam 1995;24(3):325–38.
- [33] Yun CB, Bahng EY. Structural identification using neural networks. Comput Struct 2000;77(1):41–52.
- [34] Yun CB, Yi JH, Bahng EY. Joint damage assessment of framed structures using a neural networks technique. Eng Struct 2001;23(5):425–35.
- [35] Huang H, Yang JN. Damage identification of substructure for local health monitoring. Smart Struct Syst 2008;4(6):795–807.
- [36] Huang CS. A study on techniques for analyzing ambient vibration measurement (II)—time series methods. Report No. NCREE-99-018, National Center for Research on Earthquake Engineering, Taipei, Taiwan; 1999 (in Chinese).
- [37] Huang CS, Su WC. Identification of modal parameters of a time invariant linear system by continuous wavelet transformation. Mech Syst Signal Process 2007;21(4):42–1664.
- [38] Daubechies I. Ten lectures on wavelets. Philadelphia: SIAM; 1992.
- [39] Huang CS. Structural identification from ambient vibration measurement using the multivariate AR model. J Sound Vib 2001;241(3):337–59.
- [40] Cole Jr. HA. Methods and apparatus for measuring the damping characteristics of a structure. United States Patent No. 3620069; 1971.
- [41] Huang CS, Yeh CH. Some properties of Randomdec signatures. Mech Syst Signal Process 1999;13(3):491–506.
- [42] Yeh SC, Cheng CP, Loh CH. Shaking table tests on scales down five-storey steel structures. Rep. No. NCREE-99-002, National Center for Research on Earthquake Engineering, Taipei, Taiwan; 1999 (in Chinese).